한국정밀공학회지 제 37 권 제 1 호 pp. 75-82
J. Korean Soc. Precis. Eng., Vol. 37, No. 1, pp. 75-82
January 2020 / 75
http://doi.org/10.7736/JKSPE.019.102
ISSN 1225-9071 (Print) / 2287-8769 (Online)

Check for updates

유한 요소 해석을 이용한 플라즈마 전자빔 재용융 공정의 적정 공정 변수 예측

Estimation of Appropriate Process Parameters for a Plasma Electron Beam Re-Melting Process Using Finite Element Analysis

빗리츄아[1], 이호진[2], 안동규[1,#]
Bih Lii Chua[1], Ho-Jin Lee[2], and Dong-Gyu Ahn[1,#]

1 조선대학교 기계공학과 (Department of Mechanical Engineering, Chosun University)
2 한국생산기술연구원 극한가공기술그룹 (Extreme Fabrication Technology Group, Korea Institute of Industrial Technology)
Corresponding Author / E-mail: smart@chosun.ac.kr, TEL: +82-62-230-7234, FAX: +82-62-230-7234
ORCID: 0000-0002-2111-300X

KEYWORDS: Finite element analysis (유한 요소 해석), Metal additive manufacturing (금속 적층 공정), Re-melting process (재용융 공정), Plasma electron beam (플라즈마 전자빔), Appropriate process parameters (적정 공정 변수)

Metal additive manufacturing using electron beam melting (EBM) process applies electron beam for heating, sintering, and melting of powders to fabricate a three-dimensional component. The component may contain residual porosity internally and may be subjected to poor surface finish externally. To improve the quality of the surface finish and densification, re-melting is conducted. The purpose of this paper was to estimate the appropriate process conditions for a plasma electron beam re-melting process using heat transfer finite element analyses (FEAs). The impact of the travel speed of table and thickness of the deposited part on temperature distributions were examined. The size of molten pool was estimated from the results of the thermal FEA. From the estimated size of molten pool, the travel speed of table and the hatch spacing between re-melting tracks are discussed and selected as the appropriate process conditions for electron beam re-melting process from the perspective of minimum overlapping region of the molten pool.

Manuscript received: June 25, 2019 / Revised: October 23, 2019 / Accepted: November 26, 2019

NOMENCLATURE

$\dot{Q}$ = Heat flux of electron beam
P = Power of electron beam
V = Travel speed of table
T_L = Thickness of deposited part
D = Effective diameter of heat flux
H = Penetration depth of heat flux
X = X-coordinate with respect to moving frame
Y = Y-coordinate with respect to moving frame
Z = Z-coordinate with respect to moving frame
α = Thermal diffusivity
T_{max} = Maximum temperature
T_m = Melting temperature of material
s = Position of beam center with respect to start point
d_{max} = Maximum depth of molten pool
w_L = Width of molten pool at depth of 0.5 mm from surface of deposited part
w_s = Hatch spacing between re-melting track

1. Introduction

Electron beam melting (EBM) is one of the important powder bed fusion (PBF) processes to fabricate metallic part.[1-4] A PBF process using a plasma electron beam has been proposed recently.[4-6] The EBM process involves sequential steps of preheating and melting during each deposition of powder layer to form three-dimensional components in a layer-by-layer manner.[2] However, the component fabricated by EBM process may contain residual porosity internally due to insufficient time for densification of melted powder.[2,7,8] Besides, the surface of melted layer is rough.[9-11] The presence of pores and surface roughness impose detrimental effect on the mechanical properties of the fabricated component. In order to improve the quality of surface finish and mechanical properties of the fabricated part, re-melting process is carried out.[12,13]

Focused plasma electron beam is applied to re-melt the deposited powder layer at a constant thickness of layer. AlMangour et al. investigated the scanning strategies of a PBF process experimentally and revealed that re-melting process reduces surface roughness and number of pores formed between scan tracks.[12] In order to control the re-melting process such that it does not excessively re-melt the deposited layer, investigation of influence of travel speed of table and thickness of deposited part on re-melting characteristics is required. Process modeling using finite element analyses (FEAs) provides a convenient solution and total quantification of thermal characteristics for investigation of a PBF process.[14]

Zäh and Lutzmann simulated an EBM process to estimate appropriate process window based on length-to-width ratio of molten pool.[15] Ning et al. developed an analytical model to estimate the temperature of single-track and multi-track scans of a PBF process.[14] Foteinopoulos et al. evaluated the temperature history of parts fabricated in PBF using two-dimensional finite difference method.[16] Shen and Chou studied the influence of powder with different porosities on temperature distributions and size of molten pool using a thermal finite element analysis (FEA) of EBM.[17] Cheng and Chou obtained the relationship of process parameters on geometry of molten pool for a EBM process using thermal FEA model and multi-variable regression method.[18] The scanning speed of electron beam is an important parameter in EBM that affect the built quality such as porosity.[7,15] However, these investigations were limited to melting process of laid powder layer instead of re-melting process of solidified layer.

A novel metal additive manufacturing process was proposed by Ahn and Lee that applied a re-melting process based on their melting process parameters.[6] In their process, a powder layer of 0.5 mm thick is laid, preheated, melted and re-melted using a plasma electron beam to form a deposited layer of nearly 0.5 mm.[6] Table that holds the specimen is moved relative to a fixed plasma electron beam. In order to improve the re-melting process, the effect of re-melting process parameters on the formation of melted pool should be investigated.

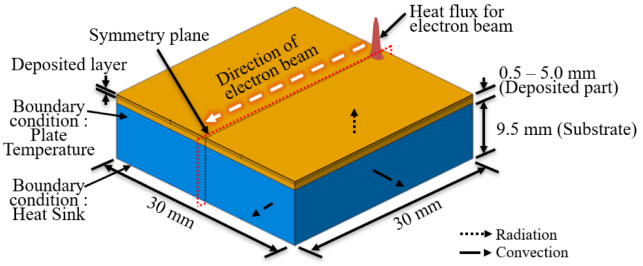

Fig. 1 Model of FEA

In this study, heat transfer analysis for a plasma electron beam re-melting process is proposed to estimate appropriate process parameters for the novel metal additive manufacturing process proposed by Ahn and Lee.[6] This is achieved by examining the effects of travel speed of table and thickness of deposited part on temperature distributions and formation of re-melted pool. Based on the estimated dimensions of re-melted pool using FEAs, appropriate process parameters such as travel speed of table and hatch distance between re-melting tracks are proposed for the plasma electron beam re-melting process.

2. Finite Element Analyses

In this study, a plasma electron beam re-melting system irradiates electron beam with power of 160 W on the specimen, which is attached to a moving table. In order to investigate the appropriate re-melting process parameters, a symmetrical three-dimensional thermal finite element model is developed, as shown in Fig. 1. Simulation of single track re-melting process using electron beam is simulated along the symmetry plane using moving heat source in Abaqus. The heat from plasma electron beam is modelled as volumetric heat flux with Gaussian distribution, given in Eq. (1).[17]

$$\dot{Q}(X,Y,Z)=\frac{16P}{\pi HD^2}\cdot\left(1-\frac{Z}{H}\right)\cdot e^{-\left[\frac{8(X^2+Y^2)}{D^2}\right]} \quad (1)$$

Table 1 lists the parameters applied in the thermal FEAs. The heat transfer analyses are carried out according to different travel speeds of table and thickness of deposited part. The effective

Table 1 Parameters of FEAs

P (W)	V (mm/s)	T_L (mm)	D (mm)	H (mm)
160	0.5-10.0	0.5-5.0	1	0.5

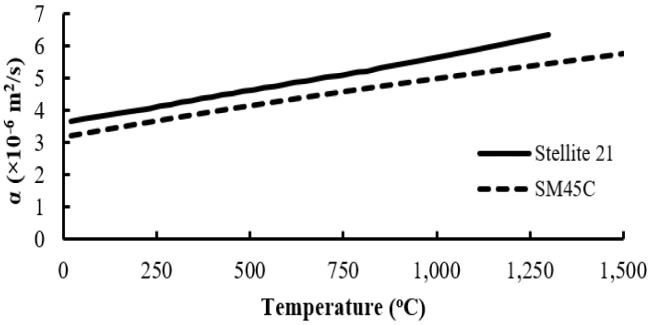

Fig. 2 Temperature dependent thermal diffusivity of SM45C steel and Stellite21 alloy[19-22]

diameter of heat flux is approximated from experiment. The penetration depth of heat flux is assumed as the thickness of laid powder.[17]

The deposited part and substrate are constructed using solid 8-node linear heat transfer elements. The materials for the substrate and the deposited part are SM45C steel and Stellite21 alloy, respectively. Unlike powder layer in melting process, the deposited part in re-melting process is assumed as solid in FEA because the porosity within the deposited part is small and its effect on thermal diffusivity can be neglected. Temperature dependent thermal diffusivity of solid SM45C steel and Stellite21 alloy are applied in the model of FEAs, as shown in Fig. 2.[19-22] The melting temperature of SM45C steel and Stellite21 are 1,520°C and 1,295°C, respectively.

The plate is preheated before re-melting process is performed. The initial temperature for plate and heat sink temperature are assumed to be 150°C and 25°C, respectively. The re-melting process requires a low pressure air environment for the plasma electron beam to operate properly.[4] Thus, the coefficient of convection from the substrate and deposited part to the surrounding of low pressure air is assigned as 1.0 W/m^2 × K.[23] Heat loss via radiation on the deposited part is estimated using Stefan-Boltzmann's law. Temperature dependent emissivity of Stellite21 alloy is applied.[24] Thickness of deposited part is assumed to remain unchanged after re-melting process.

3. Results and Discussion

3.1 Temperature Distributions

Figs. 3-5 show temperature distributions of specimens obtained from the three-dimensional transient heat transfer FEAs. The results of temperature distributions reveal that overall temperatures on the specimen change according to different thickness of deposited part and travel speed of table.

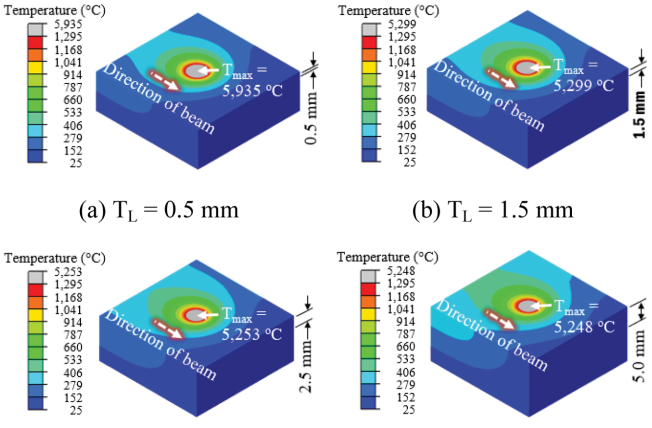

(a) T_L = 0.5 mm (b) T_L = 1.5 mm

(c) T_L = 2.5 mm (d) T_L = 5.0 mm

Fig. 3 Temperature distributions on specimens (V = 0.5 mm/s)

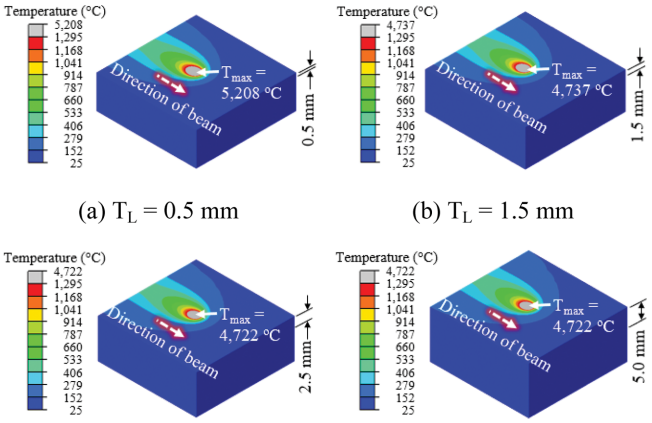

(a) T_L = 0.5 mm (b) T_L = 1.5 mm

(c) T_L = 2.5 mm (d) T_L = 5.0 mm

Fig. 4 Temperature distributions on specimens (V = 5.0 mm/s)

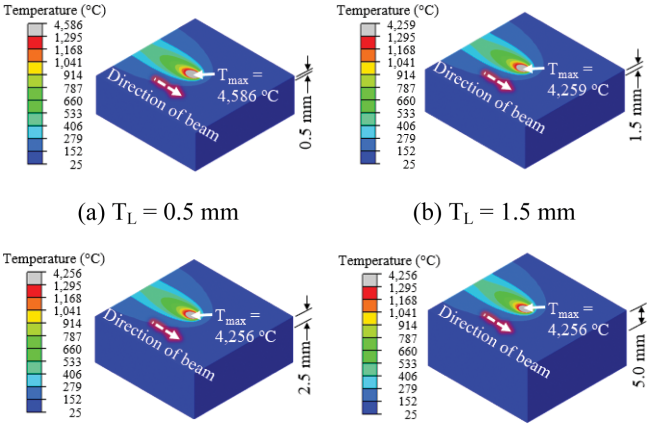

(a) T_L = 0.5 mm (b) T_L = 1.5 mm

(c) T_L = 2.5 mm (d) T_L = 5.0 mm

Fig. 5 Temperature distributions on specimens (V = 10.0 mm/s)

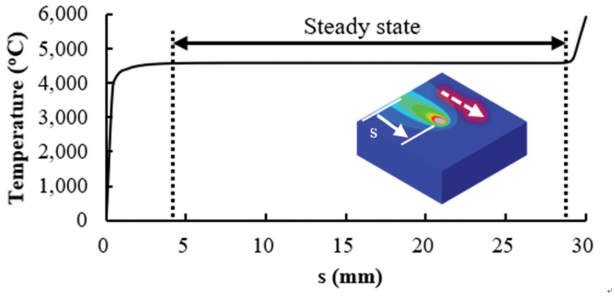

Fig. 6 Temperatures measured at the position of beam center during re-melting process (T_L = 0.5 mm and V = 10 mm/s)

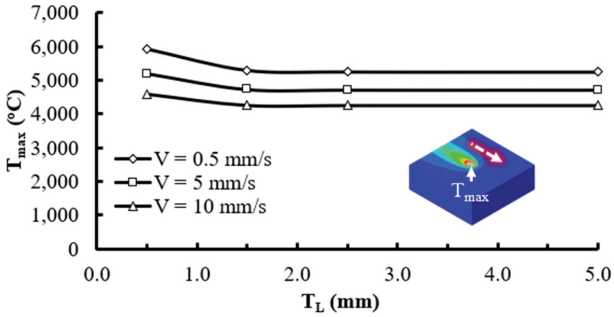

Fig. 7 Maximum temperature measured during steady state according to different thicknesses of deposited part

In order to determine the position of the steady state condition, a re-melting process with highest travel speed of table of 10 mm/s is investigated because it has the most transient condition. During re-melting process, the position of beam center is changed according to the movement of table. The temperature at the position of beam center is estimated using FEAs during re-melting process, as shown in Fig. 6. The measured temperature at the position of beam center increases rapidly during the beginning of re-melting process. The temperature converged to steady state after the beam center travelled more than 4 mm from the start position of the specimen, as shown in Fig. 6. The temperature at the position of beam center further increased from the steady state after it moved more than 28 mm because it is near to the edge of specimen. From these observations, widths and depths of molten pool during steady state condition can be properly estimated when the beam center is located at the middle of specimen for all cases of study, which is 15 mm from the start position of the specimen.

Fig. 7 shows that maximum temperature of the specimen measured during steady state condition. It reveals that temperatures reduce to a converged value as the thickness of deposited part increases. This is attributed to Stellite21 alloy has higher thermal diffusivity than SM45C steel. The maximum temperature decreases due to increase heat dissipation within the higher volume of deposited part of Stellite21 alloy. The thermal characteristics converged when the thickness of layer further increases because

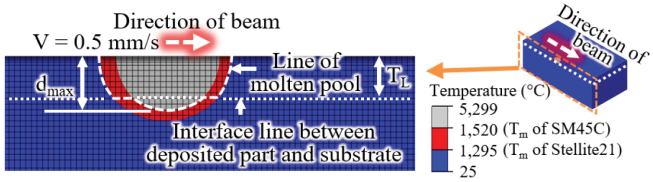

(a) Interface line between deposited part and substrate lies across temperature region greater than 1,520°C

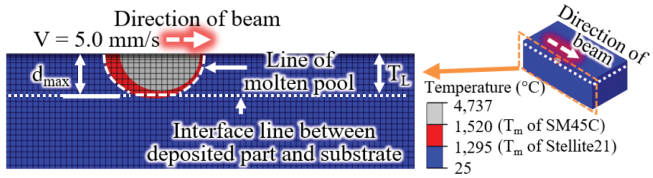

(b) Interface line between deposited part and substrate lies across temperature region range between 1,295°C-1520°C

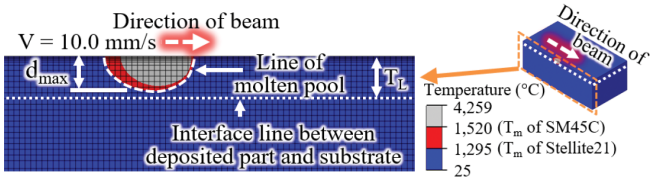

(c) Interface line between deposited part and substrate lies across temperature region less than 1,295°C

Fig. 8 Estimation of depth of molten pool based on melting temperature of different materials (T_L = 1.5 mm)

major heat transfer occurs within the deposited part of same material without being influenced by the substrate.

From Fig. 7, it shows that maximum temperature is lower when the travel speed of table is higher. This is due to reduction of energy density when the travel speed of table increases. Energy density refers to amount of heat energy per unit time.

3.2 Depth of Molten Pool

From the results of temperature distributions, the depth of molten pool is estimated based on the melting temperatures of respective materials, as depicted in Fig. 8. Both deposited part and substrate are re-melted when the depth of molten pool is greater than the thickness of deposited part. In this case, melting thickness of deposited part greater than the depth of molten pool, the melting temperature of Stellite21 is used as reference temperature of SM45C steel is applied as reference temperature to determine the depth of molten pool. For the case of specimen with temperature. In the case of depth of molten pool estimated using temperature of Stellite21 is greater than the thickness of deposited part, the depth of molten pool is set to be the thickness of deposited part. This is because the estimated temperature is not high enough to melt the substrate.

Fig. 9 shows the depth of molten pool is greater when the travel

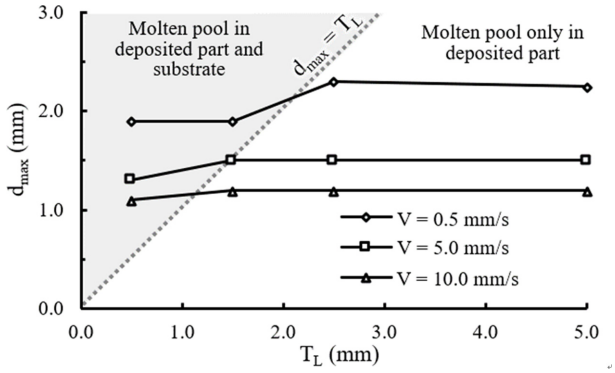

Fig. 9 Estimated depth of molten pool according to different thicknesses of deposited part

speed of table is low due to higher temperature on specimen. At the same travel speed of table, depths of molten pool are higher for those cases of molten pool only found within the deposited part as compared to those cases that molten pool penetrates the substrate. This is mainly due to the deposited part has higher thermal diffusivity than the substrate. The depth of molten pool is constant when molten pool only occurs in deposited part, regardless of thickness of deposited part. This is consistent with the observation that temperature is converged when the thickness of deposited part augments.

From Fig. 9, it is observed that travel speeds of table between 5 to 10 mm/s produces molten pool with depth in the range of 1.2 to 1.5 mm. This indicates that only two to three layers of consolidated powder are re-melted. A 0.5 mm thick of powder layer is laid during each melting process. Therefore, re-melting process using travel speeds of table between 5 to 10 mm/s are suggested as the appropriate process parameter from the viewpoint of number of re-melted layers of consolidated powder. Excessive re-melting is not encouraged because it may cause lost of material via evaporation, even though it can produce deeper molten pool.

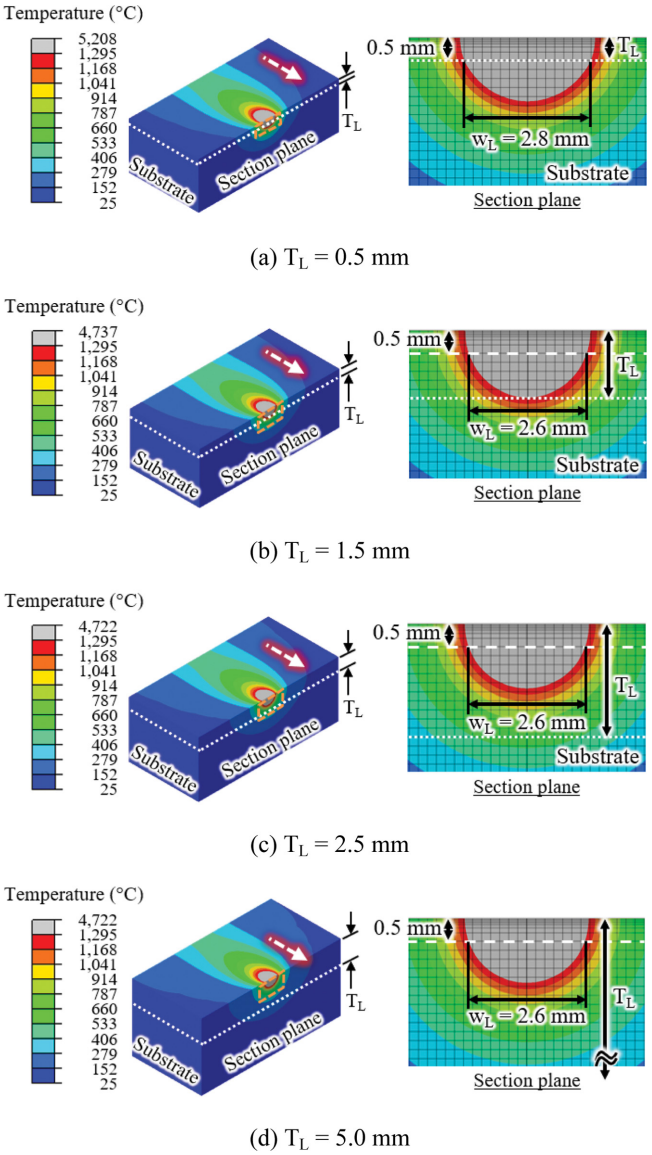

Fig. 10 Estimation of width of molten pool at depth of 0.5 mm from the surface of deposited part from temperature distribution (V = 5.0 mm/s)

3.3 Width of Molten Pool

From the results of temperature distributions, widths of molten pool at depth of 0.5 mm from the surface of deposited part are estimated based on the melting temperature of Stellite21, as shown in Fig. 10. The width estimated at depth of 0.5 mm from the surface of deposited part is discussed because it is the smallest width of molten pool within the thickness of one deposited layer on a deposited part.

Fig. 11 illustrates the influence of travel speed of table and thickness of deposited part on the formation of width of molten pool at depth of 0.5 mm from the surface of deposited part during re-melting process. The width of molten pool is higher for slower travel speed of table due to higher energy density during irradiation of electron beam. This can be observed with the increase of maximum temperature when re-melting is at slower travel speed of table, as shown in Fig. 7.

Besides, the width of molten pool reduces when the thickness of deposited part augments during re-melting process using the same travel speed of table. This is attributed to the fact that heat conduction in the horizontal directions of the deposited part is faster than in the vertical direction towards the substrate when the deposited part is thin because substrate with SM45C steel has lower thermal diffusivity than Stellite21 alloy. The width of molten pool converges when thickness of deposited part approaches to 2.5 mm for the same travel speed of table.

Re-melting using hatch spacing larger than the converged width

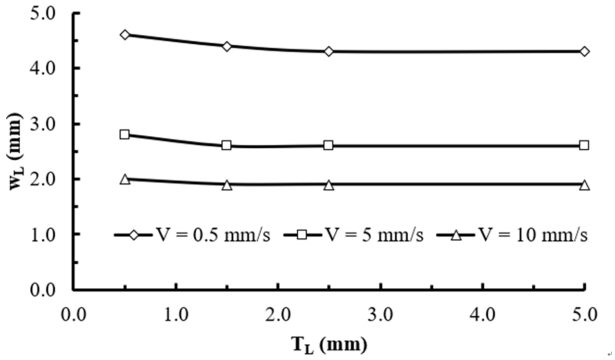

Fig. 11 Estimated width of molten pool according to different thicknesses of deposited part

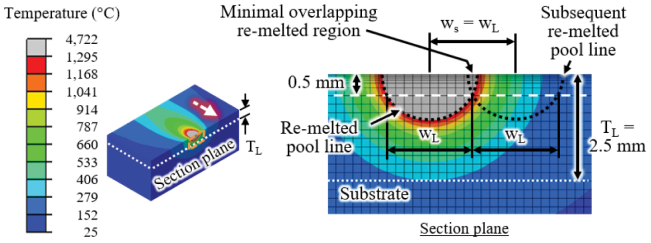

Fig. 12 Proposed appropriate hatch spacing between re-melting tracks

Table 2 Selected process parameters for plasma electron beam re-melting process

P (W)	V (mm/s)	ws (mm)
160	5.0	2.6
160	10.0	1.9

of molten pool will result in some regions of deposited part not being re-melted due to no overlapping region between re-melting tracks. Hence, it is proposed that the converged width of molten pool with respect to the travel speed of table is applied as the appropriate hatch spacing between re-melting tracks to ensure re-melting is thorough for the whole surface of deposited part with minimal overlapping region, as illustrated in Fig. 12. The appropriate travel speed of table and hatch spacing between re-melting tracks are suggested, as listed in Table 2.

4. Conclusions

In this paper, the influences of different travel speeds of table and thicknesses of deposited part on temperature distributions and formations of molten pool during re-melting process were investigated using FEAs in order to select appropriate process parameters for a plasma electron beam re-melting process. From the results of heat transfer FEAs, it was revealed that temperature distributions of deposited part were affected by travel speed of table and thickness of deposited part. The formation of molten pool was estimated from the temperature distribution using melting temperatures of deposited part and substrate. The depth and width of molten pool changed according to thickness of deposited part and converged when thickness of deposited part is greater than 2.5 mm.

Based on the above results, the appropriate travel speeds of table between 5 to 10 mm/s were suggested for the plasma electron beam re-melting process. The hatch spacing between re-melting tracks based on converged width of molten pool was determined to be appropriate process parameters for the plasma electron beam re-melting process. The suggested range of travel speeds of table is coincident with the travel speed of 5 mm/s applied for a proper deposition and re-melting process in the novel metal additive manufacturing by Ahn and Lee.[6] However, they derived the hatch spacing of 1 mm based on the width of single deposition bead.[6] The re-melting process in the novel metal additive manufacturing can be accelerated by applying the proposed hatch spacing between re-melting tracks because the proposed hatch spacing is 2.6 times larger as compared to those applied by Ahn and Lee at travel speed of 5 mm/s.

In the future, re-melting process using the suggested process parameters should be performed experimentally to validate the results of FEAs. In order to further improve the re-melting process, the effect of power and effective diameter of electron beam on the formation of re-melting pool can be considered via experiment and numerical analysis to obtain a desired wide and shallow re-melted pool.

ACKNOWLEDGEMENT

This work was supported by the National Research Foundation of Korea (NRF) grant funded by the Korea Government (MSIT) (NRF-2019R1A2C1006741).

REFERENCES

1. Bassoli, E., Sola, A., Celesti, M., Calcagnile, S., and Cavallini, C., “Development of Laser-Based Powder Bed Fusion Process Parameters and Scanning Strategy for New Metal Alloy Grades: A Holistic Method Formulation,” Materials, Vol. 11, No. 12, p. 2356, 2018.

2. Murr, L. E., Martinez, E., Amato, K. N., Gaytan, S. M., Hernandez, J., et al., “Fabrication of Metal and Alloy Components by Additive Manufacturing: Examples of 3D

Materials Science," Journal of Materials Research and Technology, Vol. 1, No. 1, pp. 42-54, 2012.

3. Chua, B. L., Lee, H. J., and Ahn, D. G., "Estimation of Effective Thermal Conductivity of Ti-6Al-4V Powders for a Powder Bed Fusion Process Using Finite Element Analysis," International Journal of Precision Engineering and Manufacturing, Vol. 19, No. 2, pp. 257-264, 2018.
4. Lee, H. J., Ahn, D. G., Song, J. G., Kim, J. S., and Kang, E. G., "Fabrication of Beads Using a Plasma Electron Beam and Stellite21 Powders for Additive Manufacturing," International Journal of Precision Engineering and Manufacturing-Green Technology, Vol. 4, No. 4, pp. 453-456, 2017.
5. Lee, H. J., Song, J. G., Kim, J. S., and Ahn, D. G., "Preliminary Study on Pre-Heating Process of Stellite21 Powder Using Electron Beam," Journal of the Korean Society for Precision Engineering, Vol. 33, No. 5, pp. 419-425, 2016.
6. Ahn, D. G. and Lee, H. J., "Investigation of Novel Metal Additive Manufacturing Process Using Plasma Electron Beam based on Powder Bed Fusion," CIRP Annals, Vol. 68, No. 1, pp. 245-248, 2019.
7. Murr, L., Gaytan, S., Medina, F., Martinez, E., Hernandez, D., et al., "Effect of Build Parameters and Build Geometries on Residual Microstructures and Mechanical Properties of Ti-6Al-4V Components Built by Electron Beam Melting (EBM)," Proc. of the 20th Annual International Solid Freeform Fabrication Symposium, pp. 374-397, 2009.
8. Liu, S. and Shin, Y. C., "Additive Manufacturing of Ti6Al4V Alloy: A Review," Materials & Design, Vol. 164, Paper No. 107552, 2019.
9. Klingvall Ek, R., Rännar, L. E., Bäckström, M., and Carlsson, P., "The Effect of EBM Process Parameters upon Surface Roughness," Rapid Prototyping Journal, Vol. 22, No. 3, pp. 495-503, 2016.
10. Safdar, A., He, H., Wei, L., Snis, A., and Chavez de Paz, L. E., "Effect of Process Parameters Settings and Thickness on Surface Roughness of EBM Produced Ti-6Al-4V," Rapid Prototyping Journal., Vol. 18, No. 5, pp. 401-408, 2012.
11. Vayssette, B., Saintier, N., Brugger, C., Elmay, M., and Pessard, E., "Surface Roughness of Ti-6Al-4V Parts Obtained by SLM and EBM: Effect on the High Cycle Fatigue Life," Procedia Engineering, Vol. 213, pp. 89-97, 2018.
12. AlMangour, B., Grzesiak, D., and Yang, J. M., "Scanning Strategies for Texture and Anisotropy Tailoring during Selective Laser Melting of TiC/316L Stainless Steel Nanocomposites," Journal of Alloys and Compounds, Vol. 728, pp. 424-435, 2017.
13. Jang, Y. H., Ahn, D. G., Kim, J., and Kim, W. S., "Re-Melting Characteristics of a Stellite21 Deposited Part by Direct Energy Deposition Process Using a Pulsed Plasma Electron Beam with a Large Irradiation Area," International Journal of Precision Engineering and Manufacturing-Green Technology, Vol. 5, No. 4, pp. 467-477, 2018.
14. Ning, J., Sievers, D., Garmestani, H., and Liang, S., "Analytical Modeling of In-Process Temperature in Powder Bed Additive Manufacturing Considering Laser Power Absorption, Latent Heat, Scanning Strategy, and Powder Packing," Materials, Vol. 12, No. 5, pp. 1-16, 2019.
15. Zäh, M. F. and Lutzmann, S., "Modelling and Simulation of Electron Beam Melting," Production Engineering Research and Development, Vol. 4, No. 1, pp. 15-23, 2010.
16. Foteinopoulos, P., Papacharalampopoulos, A., and Stavropoulos, P., "On Thermal Modeling of Additive Manufacturing Processes," CIRP Journal of Manufacturing Science and Technology, Vol. 20, pp. 66-83, 2018.
17. Shen, N. and Chou, K., "Thermal Modeling of Electron Beam Additive Manufacturing Process-Powder Sintering Effects," Proc. of the ASME International Manufacturing Science and Engineering Conference on American Society of Mechanical Engineers Digital Collection, pp. 289-295, 2012.
18. Cheng, B. and Chou, K., "Melt Pool Geometry Simulations for Powder-Based Electron Beam Additive Manufacturing," Proc. of the 24th Annual International Solid Freeform Fabrication Symposium, pp. 644-654, 2013.
19. Farwick, D. and Johnson, R., "Thermophysical Properties of Selected Wear-Resistant Alloys," Hanford Engineering Development Laboratory, Technical Report, HEDL-TME-79-6, 1980.
20. Touloukian, Y. S., Powell, R. W., Ho, C. Y., and Klemens, P. G., "Thermophysical Properties of Matter Volume 1: Thermal Conductivity-Metallic Elements and Alloys," IFI/Plenum, 1970.
21. Touloukian, Y. S. and Buyco, E. H., "Thermophysical Properties of Matter Volume 4: Specific Heat-Metallic Elements and Alloys," IFI/Plenum, 1970.
22. Touloukian, Y. S., Powell, R. W., Ho, C. Y., and Nicolaou, M. C., "Thermophysical Properties of Matter Volume 10: Thermal Diffusivity-Metallic Elements and Alloys," IFI/Plenum, 1973.
23. Saidi, M. and Abardah, R. H., "Air Pressure Dependence of Natural-Convection Heat Transfer," Proc. of the World Congress on Engineering, Vol. 2, pp. 1444-1447, 2010.
24. Touloukian, Y. S. and DeWitt, D. P., "Thermophysical Properties of Matter Volume 7: Thermal Radiative Properties-Metallic Elements and Alloys," IFI/Plenum, 1970.

Bih Lii Chua
He is Ph.D. candidate in the Department of Mechanical Engineering, Chosun University. His research interests are modeling and simulation of metal additive manufacturing using laser and electron beam.
E-mail: bihlii.chua@gmail.com

Ho-Jin Lee
He is senior researcher at the Extreme Fabrication Technology Group, Korea Institute of Industrial Technology. He received Ph.D. degree from Chosun University, Korea in 2018. His research interest includes development, application and numerical analysis of a metal additive manufacturing process.
E-mail: hlee3@kitech.re.kr

Dong-Gyu Ahn
He is Professor at the Department of Mechanical Engineering, Chosun University. He received his M.S. and Ph.D. degrees from KAIST, Korea in 1994 and 2002, respectively. His research interests include development and application of 3D printing technology, rapid manufacturing, lightweight sandwich, and mold and die.
E-mail: smart@chosun.ac.kr